RSC Advances

PAPER

View Article Online
View Journal | View Issue

Cite this: *RSC Adv.*, 2020, **10**, 6460

Photostable near-infrared-absorbing diradical-platinum(II) complex solubilized by albumin toward a cancer photothermal therapy agent†

Ryota Sawamura, Masataka Sato, Atsuko Masuya-Suzuki and Nobuhiko Iki *

Received 11th December 2019
Accepted 3rd February 2020

DOI: 10.1039/d0ra00652a

rsc.li/rsc-advances

A hydrophobic diradical-platinum(II) complex was solubilized in aqueous solutions by using bovine serum albumin and exhibited photothermal conversion under near-infrared (NIR) light irradiation. The complex was introduced into cancer cells and induced cell death upon absorption of NIR. These results imply that the complex can function as a photothermal therapeutic agent.

Introduction

Recently, photothermal therapy (PTT) has attracted attention as a potential new cancer therapy to complement conventional methods such as surgery, chemotherapy, and radiotherapy.[1] PTT utilizes near-infrared radiation (NIR, 700–1100 nm) to penetrate biological tissue with minimal damage to normal cells. NIR-absorbing photothermal agents that convert the energy of NIR light into heat can kill cancer cells. If the agents are delivered selectively to cancer cells, heat generation is localized and results in minimal damage to the surrounding tissue. Multiple NIR-absorbing materials have been studied as PTT agents, such as gold nanostructures,[2] carbon nanomaterials,[3] quantum dots,[4] and semiconducting polymers.[5] In particular, small-molecule cyanine dyes (indocyanine green (ICG), IR825, *etc.*) are often used because of their high biocompatibility.[6] Cyanine dyes show NIR absorption by the low energy gap between S_0–S_1 derived from the extended π electron system. However, the photosensitizing property of these dyes towards O_2 molecules results in autocleavage and photobleaching.[7] Even if stored in the dark, cyanine dyes are easily oxidized and cleaved.[8] In addition, the fluorescence of these dyes is disadvantageous because a substantial portion of the energy absorbed as light is emitted as fluorescence and not as heat. Therefore, optical properties of cyanine dyes decrease the efficiency of photothermal conversion.

With the aim of developing new photothermal agents, we have studied a series of diradical-platinum(II) complexes consisting of two *o*-diiminobenzosemiquinonate radical ligands and Pt^{II}.[9] These complexes absorb NIR light in the region of 700–800 nm with high intensity ($\varepsilon \approx 10^5\ M^{-1}\ cm^{-1}$) by ligand-to-ligand charge transfer.[10] Water-soluble diradical complexes have been synthesized as NIR-absorbing bioimaging probes. However, there is a concern that platinum complexes might dissociate through ligand substitution by a bio-thiol, glutathione, which is present in the cytosol at high concentration (0.5–10 mM).[11] To avoid dissociation, the complex needs to be introduced into hydrophobic regions of cells such as the cytoplasmic membrane. Past reports indicate that the uncharged complex containing bromo groups (**PtL_2**, Scheme 1) does not show NIR absorption in aqueous solution but does show NIR absorption in hydrophobic environments such as liposome bilayers.[12] Moreover, **PtL_2** does not exhibit fluorescence, suggesting it has a high efficiency of photothermal conversion. Based on these past results, we expected that **PtL_2** might be localized in cellular membranes in cancer cells and could cause cell death by its photothermal effect.

Here we report that the complex **PtL_2** can serve as a new small-molecule PTT agent that may replace low photostability organic dyes. The complex solubilized by bovine serum albumin (BSA) was introduced into cancer cells and under NIR laser irradiation, the cells were killed by the photothermal effect of solubilized **PtL_2**.

Results and discussion

The diradical complex **PtL_2** was synthesized by two steps (Scheme S1†). The first step was the complexation between Pt^{II} and 3,5-dibromo-1,2-diaminobenzene (H_2L). Heating the

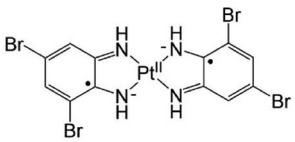

Scheme 1 Chemical structure of **PtL_2**.

Graduate School of Environmental Studies, Tohoku University, 6-6-07, Aramaki-Aoba, Aoba-ku, Sendai, 980-8579, Japan. E-mail: iki@tohoku.ac.jp; Fax: +81-22-795-7293

† Electronic supplementary information (ESI) available: Experimental details and supporting data on the solubilization of **PtL_2**, stability against NIR laser irradiation of ICG and cytotoxicity of solubilized **PtL_2**. See DOI: 10.1039/d0ra00652a

reaction mixture under Ar atmosphere afforded $[Pt(H_2L)_2]^{2+}$ without causing deprotonation or oxidation of H_2L ligands. Since the obtained complex $[Pt(H_2L)_2]^{2+}$ was water-soluble, it was successfully separated from insoluble unreacted starting materials by filtration. In the second step, heating the filtrate in the presence of air promoted the deprotonation and oxidation of the ligands from phenylene H_2L to semiquinonate L^-. Following this step, blue-violet **PtL_2** crystals were obtained. The complex showed maximum absorption at 736 nm in dimethyl sulfoxide (DMSO) with the ε value of 1.3×10^5 M^{-1} cm^{-1} (Fig. 1a, dashed line).

Next, we studied solubilization of the hydrophobic **PtL_2** by using BSA, a known hydrophilic lipid carrier protein. Absorption spectra of mixtures of **PtL_2** in DMSO and BSA in phosphate buffer saline (PBS) at different **PtL_2**/BSA molar ratios (5 : 1–1 : 5) were measured after heating at 37 °C for 24 h. As the concentration of BSA increased, the absorbance at around 650 nm decreased and that at 740 nm increased (Fig. S1†). When the **PtL_2**/BSA molar ratio was >1, violet precipitates formed in solution. These results suggest that **PtL_2** was in equilibrium between the insoluble aggregates (absorption band at around 650 nm) and the solubilized form (absorption band at 740 nm). Excess BSA shifted the equilibrium to the solubilized form, suggesting that the hydrophobic cavity of BSA accommodated **PtL_2** (ref. 9*c*) thereby increasing solubility. Presence of the equilibrium between aggregated and BSA-bound **PtL_2** was further confirmed by measuring dynamic light scattering (DLS) of the solution (Fig. S2†). With **PtL_2**/BSA molar ratio > 0.5, particles with 10^{-6}–10^{-5} m diameters can be seen. But in the presence of 20-fold amount of BSA against **PtL_2**, peaks assignable to particles were not shown. Establishment of the equilibrium took 8 h as measured by the temporal change of the absorption spectra (Fig. S3a†). Following ultrafiltration to remove DMSO, the obtained PBS solution also exhibited NIR absorption (Fig. 1a, solid line). Therefore, **PtL_2** was successfully solubilized in PBS by using BSA without organic solvents.

Long-term stability of the PBS solution of **PtL_2** was evaluated from the temporal change of absorption spectra at 4 °C. The absorbance at 740 nm of the solution decreased by *ca.* 30% over one week (Fig. 1b). Additionally, the proportion of absorption measured at the shorter wavelength increased (Fig. S4†). These results suggest that storage at 4 °C for a week shifted the equilibrium of **PtL_2** species from the solubilized form to the aggregate form. Aggregates were solubilized by re-heating at 37 °C for 4 h as confirmed by the restoration of the absorption spectrum to the original one (Fig. S5†).

To confirm whether solubilized **PtL_2** can exhibit photothermal effect and photostability, the temperature of PBS solutions of **PtL_2** was measured under irradiation by 730 nm laser (2 W cm^{-2}) for 30 min. Temperature change (ΔT, from initial temperature) of the solution increased over time (Fig. 1c) with samples containing higher concentration of the complex showing larger ΔT. For example, at 40 μM **PtL_2**, the solution temperature increased by 17.7 °C. By contrast, in PBS only, the temperature increased by only 0.8 °C. Notably, the absorption spectrum of the PBS solution of the complex was almost unchanged after 30 min irradiation by NIR (Fig. 1d). This implies that the complex remained in the solubilized form without decomposition during irradiation. We compared these results to one using 5.0 μM ICG in PBS (Fig. S6a†). The temperature reached a maximum at *ca.* 750 s and then decreased gradually. After the irradiation, NIR absorption of the ICG solution greatly diminished (Fig. S6b†). ICG is decomposed under the effects of singlet oxygen generated by the energy transfer from the triplet excited state of ICG to triplet oxygen.[13] This suggests that the temperature decrease of the ICG solution after 450 s was caused by a decrease in the number of remaining ICG molecules under NIR irradiation. We further studied the photostability of **PtL_2** upon laser irradiation by photothermal cycle experiment (Fig. S7a†). As can be seen, **PtL_2** showed increase and decrease in the solution temperature upon irradiation on and off, respectively. The three cycles seemed to be very similar, suggesting high photostability of **PtL_2**. By contrast, in the same experiment, ICG solution showed that the increase and decrease in the first cycle were not re-produced in the following cycles with diminished temperature changes (Fig. S7b†), suggesting very poor photostability. Therefore, our results suggest that unlike ICG, **PtL_2** solubilized in PBS can generate heat without decomposition upon NIR laser irradiation.

With positive results regarding the photothermal conversion ability and photostability of solubilized **PtL_2**, we introduced the solubilized complex into cancer cells. Human breast cancer cell line MCF-7 was incubated in culture medium containing the solubilized complex (20 μM) for 2 h. The pseudo color image of the cells obtained with a spectral camera showed light blue color (Fig. 2a). The absorption spectrum of the colored area (black frame region) in Fig. 2a was almost the same as that of the complex solubilized in PBS (Fig. 2b). The region showing the

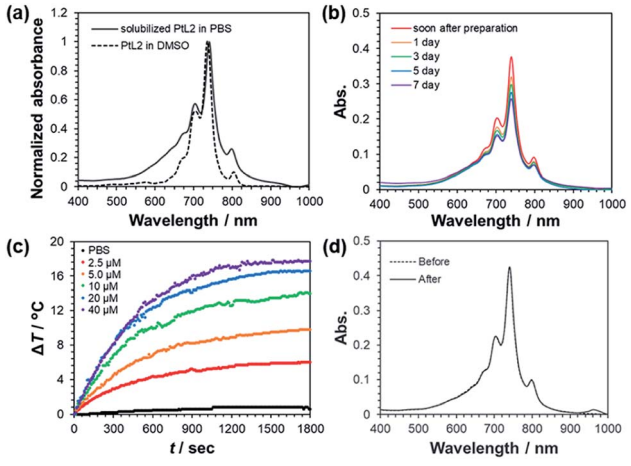

Fig. 1 (a) Absorption spectra of 2.5 μM PBS solution of **PtL_2** (solid line) and 10 μM **PtL_2** in DMSO (dashed line) normalized by absorbance at each maximum absorption wavelength. (b) The temporal change of absorption spectra of 5.0 μM **PtL_2** solubilized in PBS for a week. (c) Temperature change of PBS solution of **PtL_2** at different concentrations under the irradiation by 730 nm laser (2 W cm^{-2}). [**PtL_2**] = 0, 2.5, 5.0, 10, 20, and 40 μM in PBS. (d) Absorption spectra of PBS solution of 5.0 μM **PtL_2** before and after irradiation of 730 nm laser light (2 W cm^{-2}) for 30 min.

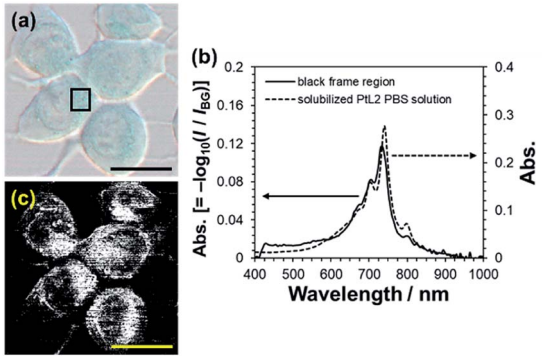

Fig. 2 (a) Pseudo color image of MCF-7 cells incubated in the culture medium containing solubilized PtL_2 (20 μM) for 2 h. (b) Absorption spectra of the black frame region in (a) (solid line, left axis) and PtL_2 solubilized in PBS (dashed line, right axis). I and I_{BG} are intensity of the transmitted light through the black flame region and background without the cells, respectively. (c) The distribution which shows the similar spectrum as the black frame region. Scale bars represent 10 μm.

NIR absorption characteristic of the complex can be depicted using a spectral angle mapper algorithm (Fig. 2c).[14] The solubilized complex showed specific subcellular localization. We then elucidated the subcellular distribution of the solubilized complex by using organelle markers (Fig. 3). The complex was not observed in nuclei but was observed in mitochondria and the endoplasmic reticulum. Therefore, solubilized **PtL_2** was successfully introduced into MCF-7 cells.

The cytotoxicity of solubilized **PtL_2** in the dark to MCF-7 cells was analyzed by Calcein AM assay. After incubation for 24 h, more than 50% of the cells containing the solubilized complex at concentration of over 10 μM had died (Fig. S8†). The half maximal inhibitory concentration (IC_{50}) value was estimated to be 8.1 μM (5.9 μg mL^{-1}). Therefore, the solubilized complex has greater cytotoxicity than conventional NIR-absorbing materials but lower cytotoxicity than conventional anti-cancer drugs (Table S1†). For biomedical applications, it would be necessary to improve the biocompatibility of the complex.

Finally, the cell-killing ability of solubilized **PtL_2** by NIR irradiation was studied over the course of an incubation time sufficiently short that dark state cytotoxicity did not occur. The

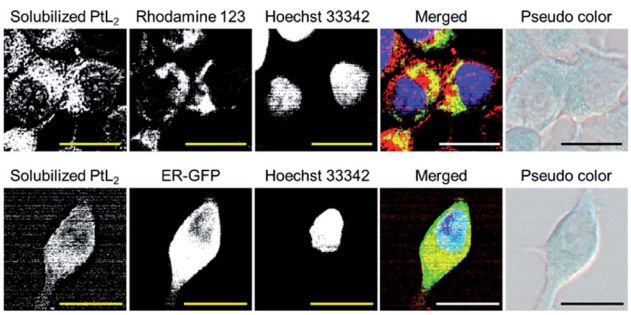

Fig. 3 Subcellular localization of solubilized PtL_2 in MCF-7 cells analyzed by using spectral angle mapper algorithm. R: the solubilized complex, G: Rhodamine 123 (mitochondria) or ER-GFP (endoplasmic reticulum), B: Hoechst 33342 (nuclei). Scale bars represent 10 μm.

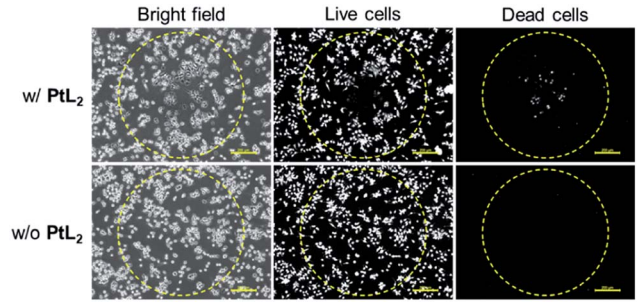

Fig. 4 Bright field and fluorescence images of live and dead MCF-7 cells with and without PtL_2 (20 μM). The cells were irradiated by 730 nm laser light (0.28 W, spot size: 1 mm) for 15 min. The dashed circle shows the laser spot. Scale bars represent 200 μm.

MCF-7 cells with or without complex were irradiated by 730 nm laser (0.28 W, spot size: 1 mm) for 15 min. Following irradiation, dead cells were observed at the center of the laser spot (Fig. 4, upper row). In contrast, live cells were observed located in the periphery of the center within the laser spot, suggesting that the irradiation power may not be high enough to kill the cells. In the control, cells without solubilized **PtL_2** survived both inside and outside the laser spot (Fig. 4, lower row). These results indicate that photothermal conversion of the diradical complex can cause cell death by NIR laser irradiation.

Conclusion

In summary, the hydrophobic complex **PtL_2** solubilized by BSA functions as a photothermal agent in aqueous environments. During irradiation by NIR laser, the complex solubilized in PBS generated heat without its degradation. In MCF-7 cells, the complex localized to mitochondria and/or endoplasmic reticulum as shown by the NIR absorption of the complex. Cancer cells containing the complex were killed by the photothermal effect of the complex under NIR laser irradiation. This study has demonstrated for the first time that diradical-platinum(II) complex can be applied as a PTT. Further study of tumor-specific delivery of **PtL_2** by using encapsulation into the amphiphilic copolymer micelles is now underway.

Conflicts of interest

There are no conflicts to declare.

Acknowledgements

This work was partly supported by JSPS KAKENHI grant number 17H03073. One of us (A. M.-S.) was supported by the Naito Foundation Subsidy for Female Researchers after Maternity Leave.

Notes and references

1 (*a*) L. Zou, H. Wang, B. He, L. Zeng, T. Tan, H. Cao, X. He, Z. Zhang, S. Guo and Y. Li, *Theranostics*, 2016, **6**, 762; (*b*)

D. Jaque, L. M. Maestro, B. del Rosal, P. Haro-Gonzalez, A. Benayas, J. L. Plaza, E. M. Rodríguez and J. G. Solé, *Nanoscale*, 2014, **6**, 9494.

2 (*a*) X. Huang, I. H. El-Sayed, W. Qian and M. A. El-Sayed, *J. Am. Chem. Soc.*, 2006, **128**, 2115; (*b*) M. R. K. Ali, Y. Wu, Y. Tang, H. Xiao, K. Chen, T. Han, N. Fang, R. Wu and M. A. El-Sayed, *Proc. Natl. Acad. Sci.*, 2017, **114**, E5655; (*c*) M. Sun, D. Peng, H. Hao, J. Hu, D. Wang, K. Wang, J. Liu, X. Guo, Y. Wei and W. Gao, *ACS Appl. Mater. Interfaces*, 2017, **9**, 10453.

3 (*a*) K. Yang, S. Zhang, G. Zhang, X. Sun, S. Lee and Z. Liu, *Nano Lett.*, 2010, **10**, 3318; (*b*) F. Zhou, D. Xing, Z. Ou, B. Wu, D. E. Resasco and W. R. Chen, *J. Biomed. Optic.*, 2009, **14**, 021009; (*c*) C. Liang, S. Diao, C. Wang, H. Gong, T. Liu, G. Hong, X. Shi, H. Dai and Z. Liu, *Adv. Mater.*, 2014, **26**, 5646.

4 (*a*) Z. Sun, H. Xie, S. Tang, X. Yu, Z. Guo, J. Shao, H. Zhang, H. Huang, H. Wang and P. K. Chu, *Angew. Chem., Int. Ed.*, 2015, **54**, 11526; (*b*) T. Yang, Y. Tang, L. Liu, X. Lv, Q. Wang, H. Ke, Y. Deng, H. Yang, X. Yang, G. Liu, Y. Zhao and H. Chen, *ACS Nano*, 2017, **11**, 1848; (*c*) G. Liang, X. Jin, H. Qin and D. Xing, *J. Mater. Chem. B*, 2017, **5**, 6366.

5 (*a*) J. Zhou, Z. Liu, X. Zhu, X. Wang, Y. Liao, Z. Ma and F. Li, *Biomaterials*, 2013, **34**, 9584; (*b*) K. Yang, H. Xu, L. Cheng, C. Sun, J. Wang and Z. Liu, *Adv. Mater.*, 2012, **24**, 5586; (*c*) Y. Lyu, C. Xie, S. A. Chechetka, E. Miyako and K. Pu, *J. Am. Chem. Soc.*, 2016, **138**, 9049.

6 (*a*) X. Song, Q. Chen and Z. Liu, *Nano Res.*, 2015, **8**, 340; (*b*) F. Xue, Y. Wen, P. Wei, Y. Gao, Z. Zhou, S. Xiao and T. Yi, *Chem. Commun.*, 2017, **53**, 6424; (*c*) G. Pan, H. Jia, Y. Zhu, R. Wang, F. Wu and Z. Chen, *ACS Biomater. Sci. Eng.*, 2017, **3**, 3596.

7 R. R. Nani, J. A. Kelley, J. Ivanic and M. J. Schnermann, *Chem. Sci.*, 2015, **6**, 6556.

8 V. Saxena, M. Sadoqi and J. Shao, *J. Pharm. Sci.*, 2003, **92**, 2090.

9 (*a*) A. Masuya, N. Iki, C. Kabuto, Y. Ohba, S. Yamauchi and H. Hoshino, *Eur. J. Inorg. Chem.*, 2010, **22**, 3458; (*b*) K. Tamura, A. Masuya, N. Iki, Y. Ohba, S. Yamauchi and H. Hoshino, *Inorg. Chim. Acta*, 2011, **378**, 81; (*c*) K. Tamura, A. Masuya, H. Hoshino and N. Iki, *Chem. Commun.*, 2013, **49**, 4812.

10 D. Herebian, K. E. Wieghardt and F. Neese, *J. Am. Chem. Soc.*, 2003, **125**, 10997.

11 S. Kemp, N. J. Wheate, M. J. Pisani and J. R. Aldrich-Wright, *J. Med. Chem.*, 2008, **51**, 2787.

12 Y. Terazono, PhD. thesis, Tohoku University, 1999.

13 E. Engel, R. Schraml, T. Maisch, K. Kobuch, B. König, R. Szeimies, J. Hillenkamp, W. Bäumler and R. Vasold, *Invest. Ophthalmol. Visual Sci.*, 2008, **49**, 1777.

14 X. Liu and C. Yang, in *Proceedings of the IEEE International Congress on Image and Signal Processing*, CISP 2013, 2013, p. 814.